Structural Engineering and Mechanics, *Vol. 69, No. 2 (2019) 145-153*
DOI: https://doi.org/10.12989/sem.2019.69.2.145

Static analysis of laminated piezo-magnetic size-dependent curved beam based on modified couple stress theory

M. Arefi*

Department of Solid Mechanic, Faculty of Mechanical Engineering, University of Kashan, Kashan 87317-51167, Iran

(Received September 27, 2018, Revised November 12, 2018, Accepted November 15, 2018)

Abstract. Modified couple stress formulation and first order shear deformation theory are used for magneto-electro-elastic bending analysis of three-layered curved size-dependent beam subjected to mechanical, magnetic and electrical loads. The governing equations are derived using a displacement field including radial and transverse displacements of middle surface and a rotation component. Size dependency is accounted based on modified couple stress theory by employing a small scale parameter. The numerical results are presented to study the influence of small scale parameter, initial electric and magnetic potentials and opening angle on the magneto-electro-elastic bending results of curved micro beam.

Keywords: modified couple stress; initial electric and magnetic potentials; bending results; radial and transverse displacements

1. Introduction

The piezoelectric materials are used in electro-mechanical systems to convert deformations or stresses to electric potential and conversely convert electric potential to deformations or stresses in sensor and actuator applications, respectively. Application of electro-mechanical systems in small scales such as micro attracted researchers for further works based on non-classical theories such as nonlocal Eringen elasticity theory, modified couple stress theory and strain gradient theory. Although combination of mentioned non-classical theories to curvilinear coordinate system such as doubly curved and curved beam leads to important issue in size-dependent analysis of structures in curvilinear coordinate system, however one can conclude that this subject has not been carefully studied. The literature review is presented to show that the subject of this paper needs some more consideration.

Petyt and Fleischer (1971) studied radial vibration analysis of a curved beam based on finite element method. The numerical results including six lowest natural frequencies of curved beam were calculated for various boundary conditions such as simply supported, hinged and clamped ends. Three dimensional analysis of a curved beam based on geometrically non-linear formulation using the total Lagrangian approach was studied by Karan *et al.* (1989). The displacement field of element was included three translations at the element nodes and thee rotations about local axes. Ibrahimbegović (1995) studied three-dimensional finite strain beam theory of Reissner based on finite element method. It was shown that an improved representation of curved reference geometry significantly increases accuracy of the results. Raveendranath *et al.* (2000) expressed some performance of curved beam finite element with coupled polynomial distributions for normal and tangential displacements that makes it possible to express the strain field in terms of only six generalized degrees of freedom leading to a simple two-node element with three degrees of freedom per node. Poon *et al.* (2002) studied nonlinear buckling responses of clamped-clamped curved beam subjected to sinusoidal excitation. The governing equations of motion were solved using Runge-Kutta numerical integration method. Kuang *et al.* (2007) investigated static responses of a circular curved beam bonded with piezoelectric actuators. The curved beam was actuated with piezoelectric layers. Bending analysis of a functionally graded piezoelectric curved beam subjected to external electric potential has been studied by Shi and Zhang (2008). Theory of piezo-elasticity has been employed for derivation of the governing equations of the model and the bending results have been derived using Taylor series expansion method. Piovan and Salazar (2015) studied dynamics of curved magneto-electro-elastic beams made from ceramic/metallic materials subjected to magneto-electric fields. They considered some advantages of this model as an element of electro-magnetic systems. The results of this problem was validated using comparison with existing references based on finite element method. Zhou *et al.* (2017) studied the transient analysis of a curved piezoelectric beam with variable curvature as piezoelectric vibration energy harvester. Two dimensional shear deformation theory was employed for electro-elastic analysis of a functionally graded piezoelectric cylindrical shell (2014). Tornabene and Ceruti (2013) investigated static and dynamic analysis of laminated doubly-curved shells and panels resting on Winkler-Pasternak elastic foundations using Generalized Differential Quadrature

*Corresponding author, Ph.D.
E-mail: arefi@kashanu.ac.ir

ISSN: 1225-4568 (Print), 1598-6217 (Online)

method based on first-order shear deformation theory. The influence of the both shell curvatures was included from the beginning of the theory formulation in the kinematic model. Validation of numerical results was performed through comparison with results of commercial programs. They mentioned that the results are in good agreement with literature. Pouresmaeeli and Fazelzadeh (2016) studied the influence of carbon nanotube reinforcement on the vibration characteristics of the thick doubly curved functionally graded composite panels. Five different patterns of carbon nanotubes along the thickness direction were used for reinforcements. First order shear deformation theory was used to derive governing equations of motion based on Hamilton's principle. The influences of volume fraction of carbon nanotubes, thickness ratio, aspect ratio and curvature ratio was studied on the responses. Free vibration analysis of a size-dependent doubly curved shell in micro scale was studied by Veysi *et al.* (2017) based on a nonlinear analysis. To account size dependency and nonlinearity in the governing equations of motion, modified couple stress theory and nonlinear Von-Karman relations were used. Multiple scales method was used to obtain an approximate analytical solution for nonlinear frequency response. Modified couple stress formulation was used for free vibration analysis of functionally graded microbeam with crack and considering damping effect by Akbas (2018). The damping effect was accounted based on Kelvin-Voigt model. Ebrahimi and Barati (2018) studied stability analysis of functionally graded piezoelectric nanobeam. To account size-dependency, the nonlocal elasticity theory was used. The effect of different external electric voltage, power-law index, nonlocal parameter and slenderness ratio was studied on the buckling loads of the size-dependent FGP nanobeams. Rahmani *et al.* (2018) studied Size dependent bending analysis of micro/nano sandwich structures based on a nonlocal high order theory. Forced vibration analysis of metal foam nanoplate with various porosities was studied based on nonlocal strain gradient theory by Barati (2017). Ehyaei and Akbarizadeh (2017) studied free vibration analysis of composite laminated beam based on modified couple stress theory. Principle of minimum potential energy was employed for derivation of governing equations of motion. The numerical results were presented in terms of material length scale parameter, beam thickness and various distributions of layers.

Tornabene *et al*. (2017) used refined shear deformation theory for free vibration analysis of laminated composite arches and beams with variable thickness. Some important works on the curved structure based on three dimensional analysis were performed by Viola *et al.* (2013) and Tornabene and Brischetto (2018).

A new shear deformation theory named four-unknown refined theory as well as modified couple stress theory were developed by Amar *et al.* (2018) for size-dependent bending and free vibration analysis of functionally graded microplate. The numerical results were presented in terms of length scale parameter based on Navier's technique. Vu-Bac *et al.* (2016) provided a sensitivity analysis for quantifying the influence of uncertain input parameters on uncertain model outputs. The effectiveness of this study were highlighted using numerical studies based on analytical functions. Hamida *et al.* (2018) provided a sensitivity analysis for identification of key input parameters affecting energy conversion factor of flexoelectric materials. The numerical results indicated that the flexoelectric constants are the most dominant factors influencing the uncertainties in the energy conversion factor. Ghasemi *et al.* (2018) presented a computational methodology for topology optimization of multi-material-based flexoelectric composites. They provided some numerical examples for two, three and four phase flexoelectric composites to demonstrate the flexibility of the model that can be obtained using multi-material topology optimization for flexoelectric composites. Some related works to optimization and computational methods of flexoelectric and piezoelectric structures were studied by various researchers (Ghasemi *et al.* 2017, Thai *et al.* 2017, Nanthakumar *et al.* 2016, Nguyen *et al.* 2018).

Author has prepared a comprehensive literature review about the important works related to some significant topics such as electro-magneto-elastic problems, size dependent analyses in micro and nano scales and curved structures. One can conclude that although some works on the curved beam have been reported by various researchers, however it is investigated that there is no comprehensive work on the electro-elastic analysis of sandwich micro curved beam subjected to electro-magneto-mechanical loads based on first order shear deformation theory and modified couple stress theory. To account size-dependency, a micro length scale parameter based on modified couple stress theory is included in constitutive relations. The governing equations are derived based on principle of virtual work. The numerical outputs such as displacements, rotation component, maximum electric and magnetic potentials are presented in terms of important parameters such as micro length scale parameter, initial electric and magnetic potentials and opening angle.

2. Size-dependency relations based on modified couple stress

The schematic of curved beam is presented in Fig. 1.

Modified couple stress formulation is used in this paper to derive size-dependent governing equations of a three-layered curved microbearn subjected to transverse loads and applied electric and magnetic potentials. The modified couple stress formulation of a curved microbeam is expressed as follows

$$U_s = \frac{1}{2}\int_V (\boldsymbol{\sigma\varepsilon} - \boldsymbol{DE} - \boldsymbol{BH} + \boldsymbol{m\chi})dV \tag{1}$$

In which $\boldsymbol{\sigma}$ and $\boldsymbol{\varepsilon}$ are the stress and strain tensors, **D** and **B** are electric displacement and magnetic induction, **E** and **H** are electric and magnetic fields, **m** is the deviatoric part of the symmetric couple stress tensor and $\boldsymbol{\chi}$ is the symmetric curvature tensor that are defined as follows

$$m = \frac{E}{1+\nu} l'^2 \chi \qquad \chi = \frac{1}{2}\left(\nabla\vec{\theta} + \left(\nabla\vec{\theta}\right)^T\right) \tag{2}$$

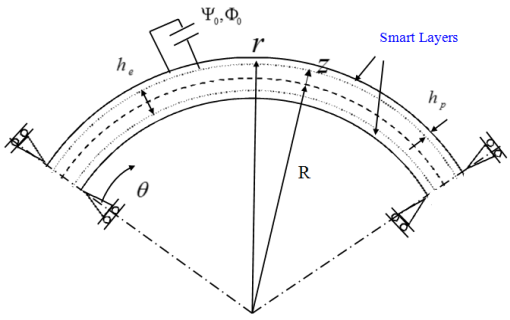

Fig. 1 The schematic figure of a three-layer curved nanobeam

In which E is modulus of elasticity, ν is Poisson ratio, l' is the material length scale parameter. In addition, θ is the rotation vector.

The stress components, electric displacement and magnetic induction are defined for the piezomagnetic materials as (Arefi and Rahimi 2011b, 2012, 2014, 2015, 2015, Arefi *et al.* 2011, 2012, Arefi and Allam 2015, Arefi and Zenkour 2017a, b, c, d)

$$\begin{aligned}\boldsymbol{\sigma} &= C\boldsymbol{\varepsilon} - e\boldsymbol{E} - q\boldsymbol{H}\\ \boldsymbol{D} &= e\boldsymbol{\varepsilon} + \epsilon\boldsymbol{E} + m\boldsymbol{H}\\ \boldsymbol{B} &= q\boldsymbol{\varepsilon} + m\boldsymbol{E} + \mu\boldsymbol{H}\end{aligned} \tag{3}$$

in which $\boldsymbol{\sigma}, \boldsymbol{\varepsilon}$ are stress and strain tensors, $\boldsymbol{E}, \boldsymbol{H}$ are electric and magnetic fields, $\boldsymbol{D}, \boldsymbol{B}$ are electric displacement and magnetic induction vectors. In addition, $C, e, \epsilon, m, q, \mu$ are elastic stiffness, piezoelectric, dielectric permittivity, magnetoelectric, piezomagnetic, and magnetic permittivity coefficients, respectively. In this stage and using the principle of virtual work $-\delta U + \delta V = 0$, we can derive the governing equations. The variation of strain energy δU and external works δV are defined as

$$\delta U = \iiint_v (\boldsymbol{\sigma}\delta\boldsymbol{\varepsilon} - \boldsymbol{D}\delta\boldsymbol{E} - \boldsymbol{B}\delta\boldsymbol{H} + \boldsymbol{m}\delta\boldsymbol{\chi})\mathrm{d}V \tag{4a}$$

$$\delta V = \iint_A (-q)\delta u_r \mathrm{d}A. \tag{4b}$$

In which q is transverse load.

Before presentation of governing equations, the electric and magnetic potentials should be defined. Electric and magnetic potentials for piezomagnetic layers are expressed as follows

$$\begin{aligned}\breve{\psi}(r,\theta) &= -\psi(\theta)\cos(\frac{\pi}{h_p}\rho) + \frac{2\psi_0}{h_p}\rho\\ \breve{\phi}(r,\theta) &= -\phi(\theta)\cos(\frac{\pi}{h_p}\rho) + \frac{2\phi_0}{h_p}\rho\end{aligned} \tag{5}$$

In which, $\psi 0$, $\phi 0$are applied electric and magnetic potentials and $\rho = \zeta \pm \frac{h_e}{2} \pm \frac{h_p}{2}$ are defined for top and bottom piezo-magnetic face-sheets. By definition of electric and magnetic potential components $(\boldsymbol{E}, \boldsymbol{H})$ using relation $(\boldsymbol{E}, \boldsymbol{H}) = -\nabla(\breve{\psi}, \breve{\phi})$, the constitutive relation can be completed.

The governing equations can be obtained by substitution of constitutive equations (Eq. (3)) into Eqs. (4) as follows

$$\begin{aligned}
\delta u_r: &-N_{\theta\theta} + \frac{dN_{r\theta}}{d\theta} + \frac{1}{4}\frac{dM_{rz}{}^{\chi}}{d\theta} + \frac{1}{4}\frac{d^2M_{\theta z}{}^{\chi}}{d\theta^2} + K_1u_r \\
&- K_2\frac{1}{r_i{}^2}\frac{d^2u_r}{d\theta^2} - q = 0\\
\delta u_\theta: &\frac{dN_{\theta\theta}}{d\theta} + N_{r\theta} + \frac{1}{4}\frac{dM_{\theta z}{}^{\chi}}{d\theta} - \frac{1}{4}M_{rz}{}^{\chi} = 0\\
\delta\chi: &\frac{dM_{\theta\theta}}{d\theta} - (RN_{r\theta} + M_{r\theta}) + M_{r\theta} - \frac{1}{2}N_{\theta\theta}{}^{\chi}\\
&+\frac{1}{4}\frac{dN_{r\theta}{}^{\chi}}{d\theta} + \frac{1}{4}M_{rz}{}^{\chi}R + \frac{1}{4}\frac{dN_{\theta z}{}^{\chi}}{d\theta} + \frac{1}{4}\frac{dP_{\theta z}{}^{\chi}}{d\theta} = 0\\
\delta\psi: &-\bar{D}_r - \frac{d\bar{D}_\theta}{d\theta} = 0\\
\delta\phi: &-\bar{B}_r - \frac{d\bar{B}_\theta}{d\theta} = 0
\end{aligned} \tag{6}$$

Substitution of resultant components in terms of basic relations into governing relations leads to

$$\begin{aligned}
\delta u_r: &-\frac{1}{4}A_{33}\frac{d^4u_r}{d\theta^4} + \left[\frac{1}{4}A_{35} + A_{11}\right]\frac{d^2u_r}{d\theta^2} - A_4u_r\\
&+\frac{1}{4}A_{33}\frac{d^3u_\theta}{d\theta^3} + \left[\frac{1}{4}A_{35} - A_4 - A_{11}\right]\frac{du_\theta}{d\theta}\\
&+\frac{1}{4}[A_{32} + A_{34}]\frac{d^3\vartheta}{d\theta^3}\\
&+\left[A_{12} - A_{13} - A_5 - \frac{1}{4}A_{35}R\right]\frac{d\vartheta}{d\theta}\\
&-A_{14}\frac{d^2\psi}{d\theta^2} - A_6\psi - A_{15}\frac{d^2\phi}{d\theta^2} - A_7\phi + K_1u_r\\
&- K_2\frac{1}{r^2}\frac{\partial^2u_r}{\partial\theta^2} - q = 0
\end{aligned}$$

$$\begin{aligned}
\delta u_\theta: &-\frac{1}{4}A_{33}\frac{d^3u_r}{d\theta^3} + \left[A_4 + A_{11} - \frac{1}{4}A_{35}\right]\frac{du_r}{d\theta}\\
&+\left[A_4 + \frac{1}{4}A_{33}\right]\frac{d^2u_\theta}{d\theta^2} - \left[A_{11} + \frac{1}{4}A_{35}\right]u_\theta\\
&+\left[A_5 + \frac{1}{4}A_{32} + \frac{1}{4}A_{34}\right]\frac{d^2\vartheta}{d\theta^2}\\
&+\left[A_{12} - A_{13} + \frac{1}{4}A_{35}R\right]\vartheta\\
&+[A_6 - A_{14}]\frac{d\psi}{d\theta} + [A_7 - A_{15}]\frac{d\phi}{d\theta} = -\frac{dN_\psi}{d\theta} - \frac{dN_\phi}{d\theta}
\end{aligned} \tag{7}$$

$$\begin{aligned}
\delta\vartheta: &-\frac{1}{4}[A_{36} + A_{33}]\frac{d^3u_r}{d\theta^3} + \left[\frac{1}{4}RA_{35} + A_5\right]\frac{du_r}{d\theta}\\
&-RA_{11}\frac{du_r}{d\theta} + \left[A_5 + \frac{1}{4}A_{33} + \frac{1}{4}A_{36}\right]\frac{d^2u_\theta}{d\theta^2}\\
&+\left[RA_{11} + \frac{1}{4}RA_{35}\right]u_\theta\\
&+\left[A_8 + \frac{1}{2}A_{32} + \frac{1}{2}A_{34} + \frac{1}{4}A_{37}\right]\frac{d^2\vartheta}{d\theta^2}\\
&+\left[-RA_{12} + RA_{13} - A_{32} - \frac{1}{4}R^2A_{35}\right]\vartheta\\
&+A_9\frac{d\psi}{d\theta} + RA_{14}\frac{d\psi}{d\theta} + A_{10}\frac{d\phi}{d\theta} + RA_{15}\frac{d\phi}{d\theta}\\
&= -\frac{dM_\psi}{d\theta} - \frac{dM_\phi}{d\theta}
\end{aligned}$$

$$\delta\psi: -A_{23}\frac{d^2u_r}{d\theta^2} - A_{16}u_r + [A_{23} - A_{16}]\frac{du_\theta}{d\theta} + [A_{25} - A_{17} - A_{24}]\frac{d\chi}{d\theta} - A_{29}\frac{d^2\psi}{d\theta^2} + A_{18}\psi - A_{30}\frac{d^2\phi}{d\theta^2} + A_{19}\phi = -D_\psi - D_\phi$$

$$\delta\phi: -A_{26}\frac{d^2u_r}{d\theta^2} - A_{20}u_r + [A_{26} - A_{20}]\frac{du_\theta}{d\theta} + [A_{28} - A_{21} - A_{27}]\frac{d\chi}{d\theta} - A_{30}\frac{d^2\psi}{d\theta^2} + A_{19}\psi - A_{31}\frac{d^2\phi}{d\theta^2} + A_{22}\phi = -B_\psi - B_\phi$$

3. Solution procedure

In this section, the solution procedure for electro-magneto-mechanical bending analysis are developed. The proposed solutions for a simply-supported curved sandwich beam are expressed as

$$\begin{Bmatrix}(u_\theta.\vartheta)\\(u_r.\psi.\phi)\end{Bmatrix} = \sum_{m=1.3.5}\begin{Bmatrix}(U_\theta.\vartheta)\cos(\alpha\theta)\\(U_r.\Psi.\Phi)\sin(\alpha\theta)\end{Bmatrix}. \quad (8)$$

in which $\alpha = {}^{m\pi R}/_{L}$. This solution indicates that two ends of curved beam are radially restricted while they can move freely along the circumferential direction. Substitution of proposed solution into governing equations leads to following well-known equation

$$[K]\{X\} = \{F\} \quad (9)$$

In which $X=\{Ur.U\theta.\mathrm{X}.\Psi.\Phi\}$ is an unknown vector corresponding to five unknown functions and $[K]$ is stiffness matrix. The elements of stiffness matrix are expressed as

$$\begin{aligned}
K_{11} &= -\tfrac{1}{4}A_{33}\alpha^4 - \left[\tfrac{1}{4}A_{35} + A_{11}\right]\alpha^2 - A_4,\\
K_{12} &= +\frac{1}{4}A_{33}\alpha^3 - \left[\frac{1}{4}A_{35} - A_4 - A_{11}\right]\alpha,\\
K_{13} &= +\frac{1}{4}[A_{32} + A_{34}]\alpha^3 - \left[A_{12} - A_{13} - A_5 - \frac{1}{4}A_{35}R\right]\alpha,\\
K_{14} &= +A_{14}\alpha^2 - A_6\,,\\
K_{15} &= +A_{15}\alpha^2 - A_7,\\
K_{21} &= \tfrac{1}{4}A_{33}\alpha^3 + \left[A_4 + A_{11} - \tfrac{1}{4}A_{35}\right]\alpha,\\
K_{22} &= -\left[A_4 + \frac{1}{4}A_{33}\right]\alpha^2 - \left[A_{11} + \frac{1}{4}A_{35}\right],\\
K_{23} &= -\left[A_5 + \frac{1}{4}A_{32} + \frac{1}{4}A_{34}\right]\alpha^2 + \left[A_{12} - A_{13} + \frac{1}{4}A_{35}R\right],\\
K_{24} &= [A_6 - A_{14}]\alpha\\
K_{25} &= [A_7 - A_{15}]\alpha,\\
K_{31} &= -\frac{1}{4}[A_{36} + A_{33}]\alpha^3 + \left[A_5 - RA_{11} + \frac{1}{4}RA_{35}\right]\alpha,\\
K_{32} &= -\left[A_5 + \frac{1}{4}A_{33} + \frac{1}{4}A_{36}\right]\alpha^2 + \left[RA_{11} + \frac{1}{4}RA_{35}\right],\\
K_{33} &= -\left[A_8 + \frac{1}{2}A_{32} + \frac{1}{2}A_{34} + \frac{1}{4}A_{37}\right]\alpha^2 + \left[-RA_{12} + RA_{13} - A_{32} - \frac{1}{4}R^2A_{35}\right],\\
K_{34} &= +[A_9 + RA_{14}]\alpha,\\
K_{35} &= (A_{10} + RA_{15})\alpha,\\
K_{41} &= +A_{23}\alpha^2 - A_{16},\\
K_{42} &= -[A_{23} - A_{16}]\alpha,\\
K_{43} &= -[A_{25} - A_{17} - A_{24}]\alpha\\
K_{44} &= +A_{29}\alpha^2 + A_{18},\\
K_{45} &= +A_{30}\alpha^2 + A_{19},\\
K_{51} &= +A_{26}\alpha^2 - A_{20}u_r,\\
K_{52} &= -[A_{26} - A_{20}]\alpha,\\
K_{53} &= -[A_{28} - A_{21} - A_{27}]\alpha\\
K_{54} &= +A_{30}\alpha^2 + A_{19},\\
K_{55} &= +A_{31}\alpha^2 + A_{22}
\end{aligned} \quad (10)$$

In addition, the elements of the force vector $\{F\}$ are expressed as

$$\begin{aligned}
F_1 &= +N_\psi + N_\phi + q\\
F_2 &= -\frac{dN_\psi}{d\theta} - \frac{dN_\phi}{d\theta}\\
F_3 &- \frac{dM_\psi}{d\theta} - \frac{dM_\phi}{d\theta}\\
F_4 &= -D_\psi - D_\phi\\
F_5 &= -B_\psi - B_\phi.
\end{aligned} \quad (11)$$

4. Results and discussions

In this section, the numerical results of the problem are presented. Before presentation of numerical results, the material properties of elastic core and piezomagnetic layers should be introduced for core and piezomagnetic layers as

Core

$$E = 1.18\,TPa \;\; v = 0.25 \quad (12)$$

Piezomagnetic face-sheets

$$\begin{aligned}
C_{\theta\theta\theta\theta}{}^p &= 286GPa \;\; C_{r\theta r\theta}{}^p = 45.3GPa\\
e_{\theta\theta r}{}^p &= e_{r\theta\theta}{}^p = -4.4(\mathrm{C/m^2})\\
e_{r\theta\theta}{}^p &= e_{\theta r\theta}{}^p = 11.6(\mathrm{C/m^2})\\
q_{\theta\theta r}{}^p &= q_{r\theta\theta}{}^p = 580.3(\mathrm{N/Am})\\
q_{r\theta\theta}{}^p &= q_{\theta r\theta}{}^p = 550(\mathrm{N/Am})\\
\epsilon_{rr}{}^p &= 9.3\times10^{-11}(\mathrm{C/mV})\\
\epsilon_{\theta\theta}{}^p &= 8\times10^{-11}(\mathrm{C/mV})\\
m_{rr}{}^p &= 3\times10^{-12}(\mathrm{Ns/CV})\\
m_{\theta\theta}{}^p &= 5\times10^{-12}(\mathrm{Ns/CV})\\
\mu_{rr}{}^p &= 1.57\times10^{-4}(\mathrm{Ns^2/C^2})\\
\mu_{\theta\theta}{}^p &= -5.9\times10^{-4}(\mathrm{Ns^2/C^2})
\end{aligned} \quad (13)$$

The electro-magneto-elastic bending results are presented in this section in terms of important parameters of the sandwich curved microbeam such as micro length scale parameter, applied electric and magnetic potentials, and

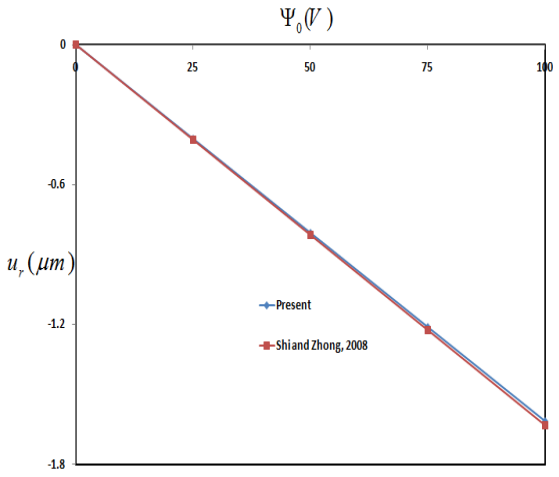

Fig. 2 Variation of radial displacement u_r in terms of applied electric potential Ψ_0

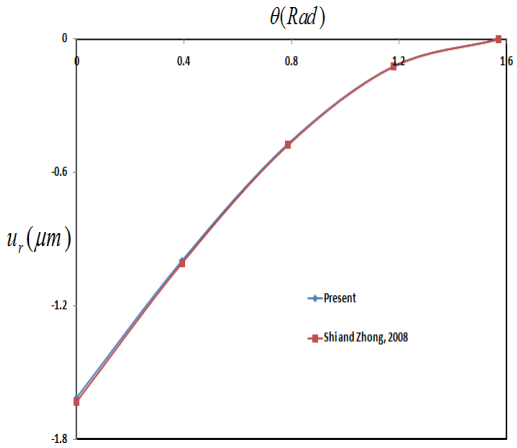

Fig. 3 Variation of radial displacement u_r in terms of angle of beam θ

opening angle. To account micro length scale parameter, a dimensionless parameter l is defined as: $l' = l \times 17.65\ \mu m$.

4.1 Comparison and validation

This section presents a comparison with previous works for validation. For this aim, reference (Shi and Zhong 2008) is used. Shown in Fig. 2 is influence of applied electric potential Ψ_0 on the variation of radial displacement u_r based on present formulation and results of Shi and Zhong (2008).

In addition, comparison between current and previous results (Shi and Zhong 2008) for radial displacement u_r in terms of angle of curved beam θ for $\Psi_0 = 100V$ is presented in Fig. 3. One can conclude that present numerical results in this paper are in good agreement with reference.

Figs. 4 and 5 show variation of dimensionless radial and transverse displacements u_r/h , u_t/h of middle surface in terms of micro length scale parameter l and opening angle $\theta = L/R$.

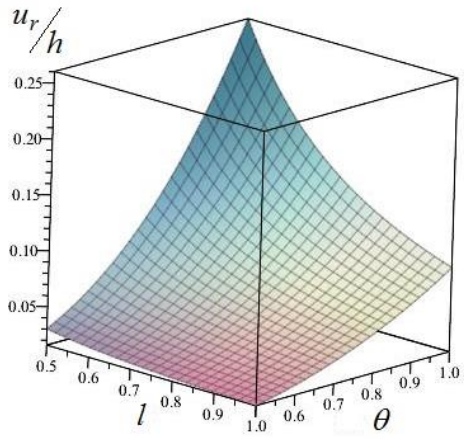

Fig. 4 Variation of dimensionless radial displacement u_r/h in terms of micro length scale parameter l and opening angle $\theta = L/R$

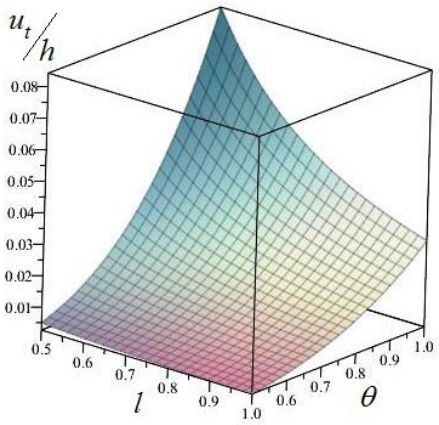

Fig. 5 Variation of dimensionless transverse displacement u_t/h in terms of micro length scale parameter l and opening angle $\theta = L/R$

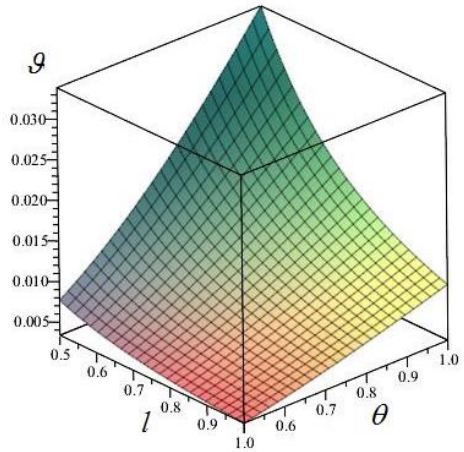

Fig. 6 Variation of rotation component ϑ in terms of micro length scale parameter l and opening angle $\theta = L/R$

One can observe that with increase of micro length scale parameter l and decrease of opening angle θ, both radial and transverse displacements are decreased significantly. It

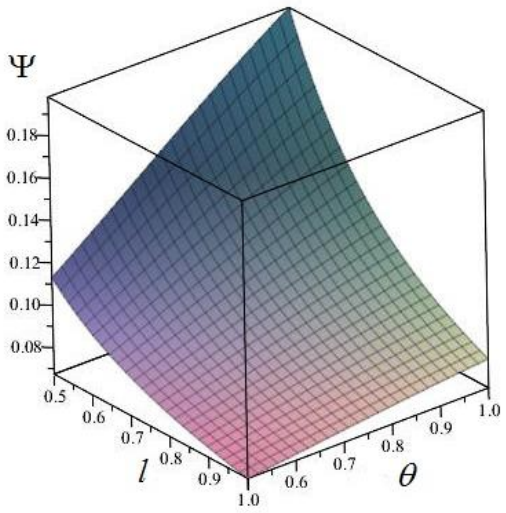

Fig. 7 Variation of maximum electric potential Ψ in terms of micro length scale parameter l and opening angle θ = L/R

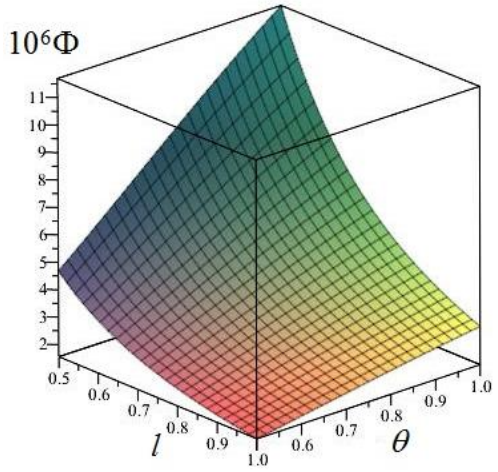

Fig. 8 Variation of maximum magnetic potential $10^6\Phi$ in terms of micro length scale parameter and opening angle θ = L/R

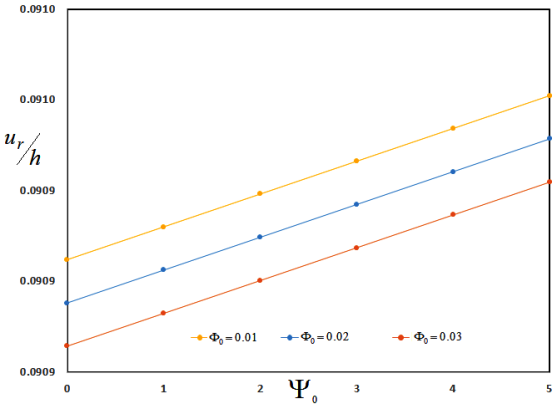

Fig. 9 Variation of dimensionless radial displacement u_r/h in terms of initial electric and magnetic potentials

can be concluded that with increase of micro length scale parameter, the stiffness of curved beam is increased and

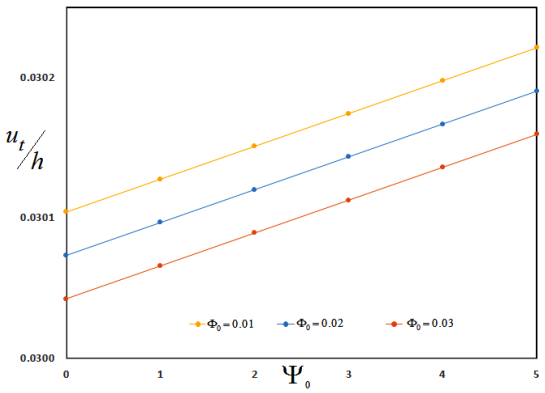

Fig. 10 Variation of dimensionless transverse displacement u_t/h in terms of initial electric and magnetic potentials

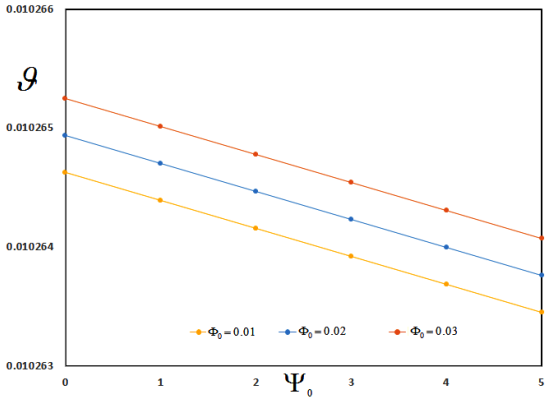

Fig. 11 Variation of rotation components ϑ in terms of initial electric and magnetic potentials

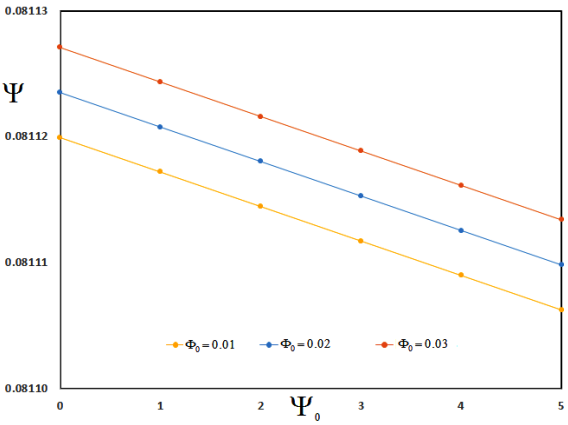

Fig. 12 Variation of maximum electric potential Ψ in terms of initial electric and magnetic potentials

consequently both displacements are decreased significantly. In addition, it is concluded that with increase of opening angle of curved beam, the stiffness is decreased and then the displacements are increased.

Shown in Fig. 6 is variation of rotation components ϑ in terms of micro length scale parameter l and opening angle θ = L/R. the same behavior concluded for Figs. 4,5 can be observed for Fig. 6.

Distribution of maximum electric and magnetic potentials through thickness direction are presented in Figs. 7, 8 in terms of micro length scale parameter l and

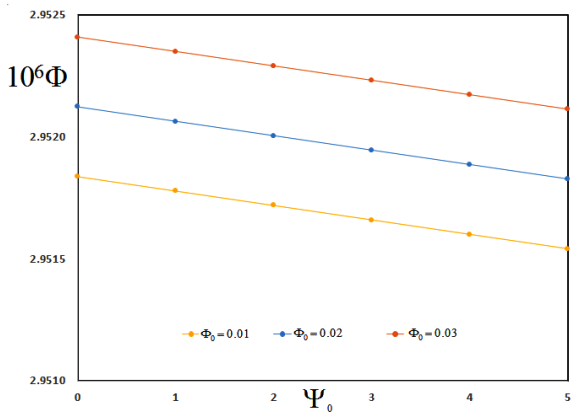

Fig. 13 Variation of maximum magnetic potential $10^6\Phi$ in terms of initial electric and magnetic potentials

opening angle $\theta = \mathrm{L/R}$, respectively. The numerical results indicate that the maximum electric and magnetic potentials through thickness direction are decreased with increase of micro length scale parameter l and decrease of opening angle θ. One can conclude that with increase of micro length scale parameter l, the stiffness of micro curved beam is increased that leads to decrease of maximum electric and magnetic potentials.

The influence of initial electric and magnetic potentials is studied on the magneto-electro-elastic results of sandwich curved microbeam. Shown in Figs. 9 and 10 are variation of dimensionless radial and transverse displacements u_r/h , u_t/h in terms of initial electric and magnetic potentials $\Psi_0.\Phi_0$. One can conclude that both displacement components are increased with increase of initial electric Ψ_0 potential and decrease of initial magnetic potential Φ_0. These conclusions are in accordance with results of previous works (Arefi and Zenkour 2017c, Arefi *et al.* 2017a, b).

Variation of rotation component, maximum electric and magnetic potentials through thickness direction is presented in Figs. 11, 12 and 13 in terms of initial electric and magnetic potentials $\Psi_0.\Phi_0$. The numerical results show that the rotation component, maximum electric and magnetic potentials are increased with increase of initial magnetic potential Φ_0 and decrease of electric potential Ψ_0.

5. Conclusions

Magneto-electro-elastic bending analysis of a three-layered curved nanobeam was studied in this paper based on modified couple stress formulation and first-order shear deformation theory.

Principle of virtual work was used to derive governing equations in terms of displacement field and magnetic and electric potentials. The numerical results were presented in terms of micro length scale parameter, opening angle, initial electric and magnetic potentials. Some significant outputs of this analysis are expressed as follows:

To account size dependency in analysis of curved microbeam, modified couple stress formulation was employed. The numerical results show that with increase of micro length scale parameter associated with this theory, the stiffness of curved microbeam is increased and consequently the displacements, rotation component, maximum electric and magnetic potentials are decreased significantly.

The opening angle as a geometric parameter has significant influence on the bending results of curved microbeam. it is concluded that with increase of opening angle of curved microbeam, the stiffness is decreased and then the displacements, rotation, maximum electric and magnetic potentials along the thickness direction are increased.

Initial electric and magnetic potentials lead to significant change of bending results. It is observed that with increase of initial electric potential and decrease of initial magnetic potential, the radial and transverse displacements are increased. In addition, it is observed that the rotation component, maximum electric and magnetic potentials are increased with increase of initial magnetic potential Φ_0 and decrease of electric potential Ψ_0.

References

Akbas, S.D. (2018), "Forced vibration analysis of cracked functionally graded microbeams", *Adv. Nano Res.*, **6**(1), 39-55.

Amar, L.H.H., Kaci, A., Yeghnem, R. and Tounsi, A. (2018), "A new four-unknown refined theory based on modified couple stress theory for size-dependent bending and vibration analysis of functionally graded micro-plate", *Steel Compos. Struct.*, **26**(1), 89-102.

Arefi, M., Kiani, M. and Zenkour, A.M. (2017b), "Size-dependent free vibration analysis of a three-layered exponentially graded nano-/micro-plate with piezomagnetic face sheets resting on Pasternak's foundation", *J. Sandw. Struct. Mater.*, **29**(5), 774-786.

Arefi, M., Zamani, M.H. and Kiani, M. (2017a), "Size-dependent free vibration analysis of three-layered exponentially graded nanoplate with piezomagnetic face-sheets resting on Pasternak's foundation", *J. Intel. Mater. Syst. Struct.*, **29**(5), 774-786.

Arefi, M. (2016), "Analysis of wave in a functionally graded magneto-electro-elastic nano-rod using nonlocal elasticity model subjected to electric and magnetic potentials", *Acta Mech.*, **227**(9), 2529-2542.

Arefi, M. and Rahimi, G.H. (2011a), "Thermo elastic analysis of a functionally graded cylinder under internal pressure using first order shear deformation theory", *Sci. Res. Essays.*, **5**(12), 1442-1454.

Arefi, M. and Zenkour, A.M. (2017a), "Employing the coupled stress components and surface elasticity for nonlocal solution of wave propagation of a functionally graded piezoelectric Love nanorod model", *J. Intel. Mater. Syst. Struct.*, **28**(17), 2403-2413.

Arefi, M. and Zenkour, A.M. (2017b), "Transient sinusoidal shear deformation formulation of a size-dependent three-layer piezo-magnetic curved nanobeam", *Acta Mech.*, **228**(10), 3657-3674.

Arefi, M. and Zenkour, A.M. (2017c), "Effect of thermo-magneto-electro-mechanical fields on the bending behaviors of a three-layered nanoplate based on sinusoidal shear-deformation plate theory", *J. Sandw. Struct. Mater.*, 1099636217697497.

Arefi, M. and Zenkour, A.M. (2017d), "Size-dependent free vibration and dynamic analyses of piezo-electro-magnetic sandwich nanoplates resting on viscoelastic foundation", *Phys.*

B: *Cond. Matt.*, **521**, 188-197.
Arefi, M. (2015), "Nonlinear electromechanical analysis of a functionally graded square plate integrated with smart layers resting on Winkler-Pasternak foundation", *Smart Struct. Syst.*, **16**(1), 195-211.
Arefi, M. and Allam, M.N.M. (2015), "Nonlinear responses of an arbitrary FGP circular plate resting on foundation", *Smart Struct. Syst.*, **16**(1), 81-100.
Arefi, M., Rahimi, G.H. and Khoshgoftar, M.J. (2011), "Optimized design of a cylinder under mechanical, magnetic and thermal loads as a sensor or actuator using a functionally graded piezomagnetic material", *Int. J. Phys. Sci.*, **6**(27), 6315-6322.
Arefi, M. and Rahimi, G.H. (2011b), "Nonlinear analysis of a functionally graded square plate with two smart layers as sensor and actuator under normal pressure", *Smart Struct. Syst.*, **8**(5), 433-447.
Arefi, M. and Rahimi, G.H. (2012), "Studying the nonlinear behavior of the functionally graded annular plates with piezoelectric layers as a sensor and actuator under normal pressure", *Smart Struct. Syst.*, **9**(2), 127-143.
Arefi, M. and Rahimi, G.H. (2014), "Comprehensive piezo-thermo-elastic analysis of a thick hollow spherical shell", *Smart Struct. Syst.*, **14**(2), 225-246.
Arefi, M., Rahimi, G.H. and Khoshgoftar, M.J. (2012), "Exact solution of a thick walled functionally graded piezoelectric cylinder under mechanical, thermal and electrical loads in the magnetic field", *Smart Struct. Syst.*, **9**(5), 427-439.
Barati, M.R. (2017), "Nonlocal-strain gradient forced vibration analysis of metal foam nanoplates with uniform and graded porosities", *Adv. Nano. Res.*, **5**(4), 393-414.
Ebrahimi, F. and Barati, M.R. (2018), "Stability analysis of functionally graded heterogeneous piezoelectric nanobeams based on nonlocal elasticity theory", *Adv. Nano. Res.*, **6**(1), 93-112.
Ehyaei, J. and Akbarizadeh, M.R. (2017), "Vibration-analysis of micro composite thin beam based on modified couple stress", *Struct. Eng. Mech.*, **64**(4), 793-802.
Ghasemi, H., Park, H.S. and Rabczuk, T. (2017), "A level-set based IGA formulation for topology optimization of flexoelectric materials", *Comput. Meth. Appl. Mech. Eng.*, **313**, 239-258.
Ghasemi, H., Park, H.S. and Rabczuk, T. (2018), "A multi-material level set-based topology optimization of flexoelectric composites", *Comput. Meth. Appl. Mech. Eng.*, **332**, 47-62.
Hamdia, K.M., Ghasemi, H., Zhuang, X., Alajlan, N. and Rabczuk, T. (2018), "Sensitivity and uncertainty analysis for flexoelectric nanostructures", *Comput. Meth. Appl. Mech. Eng.*, **337**, 95-109.
Ibrahimbegović, A. (1995), "On finite element implementation of geometrically nonlinear Reissner's beam theory three-dimensional curved beam elements", *Comput. Meth. Appl. Mech. Eng.*, **122**(1-2), 11-26.
Kuang, Y.D., Li, G.Q., Chen, C.Y. and Min, Q. (2007), "The static responses and displacement control of circular curved beams with piezoelectric actuators", *Smart Mater. Struct.*, **16**(4), 1016-1024.
Nanthakumar, S.S., Lahmer, T., Zhuang, X., Zi, G. and Rabczuk, T. (2016), "Detection of material interfaces using a regularized level set method in piezoelectric structures", *Inv. Prob. Sci. Eng.*, **24**(1), 153-176.
Nguyen, B.H., Nanthakumar, S.S., Zhuang, X., Wriggers, P. and Rabczuk, T. (2018), "Dynamic flexoelectric effect on piezoelectric nanostructures", *Eur. J. Mech. A. Sol.*, **81**, 40.
Petyt, M. and Fleischer, C.C. (1971), "Free vibration of a curved beam", *J. Sound Vibr.*, **18**(1), 17-30.
Piovan, M.T. and Olmedo Salazar, J.F. (2015), "A 1D model for the dynamic analysis of magneto-electro-elastic beams with curved configuration", *Mech. Res. Com.*, **67**, 34-38.
Poon, W.Y., Ng, C.F. and Lee, Y.Y. (2002), "Dynamic stability of a curved beam under sinusoidal loading", *Proc. Inst. Mech. Eng. Part G: J. Aer. Eng.*, **216**(4), 209-217.
Pouresmaeeli, S. and Fazelzadeh, S.A. (2016), "Frequency analysis of doubly curved functionally graded carbon nanotube-reinforced composite panels", *Acta. Mech.*, **227**(10), 2765-2794.
Rahmani, O., Deyhim, S. and Hosseini, S.A.H. (2018), "Size dependent bending analysis of micro/nano sandwich structures based on a nonlocal high order theory", *Steel Compos. Struct.*, **27**(3), 371-388.
Raveendranath, P., Singh, G. and Pradhan, B. (2000), "Free vibration of arches using a curved beam element based on a coupled polynomial displacement field", *Comput. Struct.*, **78**(4), 583-590.
Shi, Z.F. and Zhang, T. (2008), "Bending analysis of a piezoelectric curved actuator with a generally graded property for the piezoelectric parameter", *Smart Mater. Struct.*, **17**(4), 045018.
Surana, K.S. and Sorem, R.M. (1989), "Geometrically non-linear formulation for three dimensional curved beam elements with large rotations", *Int. J. Numer. Meth. Eng.*, **28**(1), 43-73.
Thai, T.Q., Rabczuk, T. and Zhuang, X. (2017), "A large deformation isogeometric approach for flexoelectricity and soft materials", *Comput. Meth. Appl. Mech. Eng.*, **341**, 718-739.
Tornabene, F. and Brischetto, S. (2018), "3D capability of refined GDQ models for the bending analysis of composite and sandwich plates, spherical and doubly-curved shells", *Thin. Wall. Struct.*, **129**, 94-124.
Tornabene, F. and Ceruti, A. (2013), "Free-form laminated doubly-curved shells and panels of revolution resting on Winkler-Pasternak elastic foundations: A 2-D GDQ solution for static and free vibration analysis", *World J. Mech.*, **3**(1), 1-25.
Tornabene, F., Fantuzzi, N. and Bacciocchi, M. (2017), "Refined shear deformation theories for laminated composite arches and beams with variable thickness: Natural frequency analysis", *Eng. Anal. Bound. Elem.*
Veysi, A., Shabani, R. and Rezazadeh, G. (2017), "Nonlinear vibrations of micro-doubly curved shallow shells based on the modified couple stress theory", *Nonlin. Dyn.*, **87**(3), 2051-2065.
Viola, E., Tornabene, F. and Fantuzzi, N. (2013), "Static analysis of completely doubly-curved laminated shells and panels using general higher-order shear deformation theories", *Compos. Struct.*, **101**, 59-93.
Vu-Bac, N., Lahmer, T., Zhuang, X., Nguyen-Thoi, T. and Rabczuk, T. (2016), "A software framework for probabilistic sensitivity analysis for computationally expensive models", *Adv. Eng. Softw.*, **100**, 19-31.
Zhou, Y., Nyberg, T.R., Xiong, G., Zhou, H. and Li, S. (2017), "Precise deflection analysis of laminated piezoelectric curved beam", *J. Intel. Mater. Syst. Struct.*, **27**(16), 2179-2198.

CC

Appendix

$$\{A_4, A_5, A_8\} = \int_{-\frac{h_e}{2}}^{+\frac{h_e}{2}} \frac{C_{\theta\theta\theta\theta}}{(R+\zeta)}\{1, z, z^2\}\mathrm{d}z + \int_{-\frac{h_e}{2}-h_p}^{-\frac{h_e}{2}} \frac{C_{\theta\theta\theta\theta}{}^p}{(R+z)}\{1, z, z^2\}\mathrm{d}z + \int_{\frac{h_e}{2}}^{\frac{h_e}{2}+h_p} \frac{C_{\theta\theta\theta\theta}{}^p}{(R+z)}\{1, z, z^2\}\mathrm{d}z$$

$$\{A_6, A_7, A_9, A_{10}\} = \int_{-\frac{h_e}{2}-h_p}^{-\frac{h_e}{2}} \frac{\pi}{h_p}\sin\left(\frac{\pi}{h_p}\rho\right)\{e_{\theta\theta r}{}^p, q_{\theta\theta r}{}^p, ze_{\theta\theta r}{}^p, zq_{\theta\theta r}{}^p\}\mathrm{d}z + \int_{\frac{h_e}{2}}^{\frac{h_e}{2}+h_p} \frac{\pi}{h_p}\sin\left(\frac{\pi}{h_p}\rho\right)\{e_{\theta\theta r}{}^p, q_{\theta\theta r}{}^p, ze_{\theta\theta r}{}^p, zq_{\theta\theta r}{}^p\}\mathrm{d}z$$

$$\{A_{11}, A_{12}, A_{13}\} = \int_{-\frac{h_e}{2}}^{+\frac{h_e}{2}} \frac{C_{r\theta r\theta}}{(R+z)}\{1, (R+z), z\}\mathrm{d}z + \int_{-\frac{h_e}{2}-h_p}^{-\frac{h_e}{2}} \frac{C_{r\theta r\theta}{}^p}{(R+z)}\{1, (R+z), z\}\mathrm{d}z + \int_{\frac{h_e}{2}}^{\frac{h_e}{2}+h_p} \frac{C_{r\theta r\theta}{}^p}{(R+z)}\{1, (R+z), z\}\mathrm{d}z$$

$$\{A_{14}, A_{15}\} = \int_{-\frac{h_e}{2}-h_p}^{-\frac{h_e}{2}} \frac{\cos\left(\frac{\pi}{h_p}\rho\right)}{(R+z)}\{e_{r\theta\theta}{}^p, q_{r\theta\theta}{}^p\}\mathrm{d}z + \int_{\frac{h_e}{2}}^{\frac{h_e}{2}+h_p} \frac{\cos\left(\frac{\pi}{h_p}\rho\right)}{(R+z)}\{e_{r\theta\theta}{}^p, q_{r\theta\theta}{}^p\}\mathrm{d}z$$

$$\{N_\psi, N_\phi, M_\psi, M_\phi\} = \int_{-\frac{h_e}{2}-h_p}^{-\frac{h_e}{2}} \{\frac{2\psi_0}{h_p}e_{\theta\theta\theta}{}^p, \frac{2\phi_0}{h_p}q_{\theta\theta\theta}{}^p, \frac{2\psi_0}{h_p}ze_{\theta\theta\theta}{}^p, \frac{2\phi_0}{h_p}zq_{\theta\theta\theta}{}^p\}\mathrm{d}z + \int_{\frac{h_e}{2}}^{\frac{h_e}{2}+h_p} \{\frac{2\psi_0}{h_p}e_{\theta\theta\theta}{}^p, \frac{2\phi_0}{h_p}q_{\theta\theta\theta}{}^p, \frac{2\psi_0}{h_p}ze_{\theta\theta\theta}{}^p, \frac{2\phi_0}{h_p}zq_{\theta\theta\theta}{}^p\}\mathrm{d}z$$

$$\{A_{16}, A_{17}, A_{20}, A_{21}\} = \int_{-\frac{h_e}{2}-h_p}^{-\frac{h_e}{2}} \frac{\pi}{h_p}\sin\left(\frac{\pi}{h_p}\rho\right)\{e_{r\theta\theta}{}^p, ze_{r\theta\theta}{}^p, q_{r\theta\theta}{}^p, zq_{r\theta\theta}{}^p\}\mathrm{d}\zeta + \int_{\frac{h_e}{2}}^{\frac{h_e}{2}+h_p} \frac{\pi}{h_p}\sin\left(\frac{\pi}{h_p}\rho\right)\{e_{r\theta\theta}{}^p, ze_{r\theta\theta}{}^p, q_{r\theta\theta}{}^p, zq_{r\theta\theta}{}^p\}\mathrm{d}z$$

$$\{A_{18}, A_{19}, A_{22}\} = \int_{-\frac{h_e}{2}-h_p}^{-\frac{h_e}{2}} (R+z)\left[\frac{\pi}{h_p}\sin\left(\frac{\pi}{h_p}\rho\right)\right]^2\{\epsilon_{rr}{}^p, m_{rr}{}^p, \mu_{rr}{}^p\}\mathrm{d}z + \int_{\frac{h_e}{2}}^{\frac{h_e}{2}+h_p} (R+z)[\frac{\pi}{h_p}\sin\left(\frac{\pi}{h_p}\rho\right)]^2\{\epsilon_{rr}{}^p, m_{rr}{}^p, \mu_{rr}{}^p\}\mathrm{d}z$$

$$\{D_\psi, D_\phi, B_\psi, B_\phi\} = \int_{-\frac{h_e}{2}-h_p}^{-\frac{h_e}{2}} (R+z)\{\frac{2\psi_0}{h_p}\epsilon_{rr}{}^p, \frac{2\phi_0}{h_p}m_{rr}{}^p, \frac{2\psi_0}{h_p}m_{rr}{}^p, \frac{2\phi_0}{h_p}\mu_{rr}{}^p\}\mathrm{d}z + \int_{\frac{h_e}{2}}^{\frac{h_e}{2}+h_p} (R+z)\{\frac{2\psi_0}{h_p}\epsilon_{rr}{}^p, \frac{2\phi_0}{h_p}m_{rr}{}^p, \frac{2\psi_0}{h_p}m_{rr}{}^p, \frac{2\phi_0}{h_p}\mu_{rr}{}^p\}\mathrm{d}z$$

$$\{A_{23}, A_{24}, A_{25}, A_{26}, A_{27}, A_{28}\} = \int_{-\frac{h_e}{2}-h_p}^{-\frac{h_e}{2}} \frac{\cos\left(\frac{\pi}{h_p}\rho\right)}{(R+z)}\begin{Bmatrix} e_{\theta r\theta}{}^p, (R+z)e_{\theta r\theta}{}^p, ze_{\theta r\theta}{}^p \\ q_{\theta r\theta}{}^p, (R+z)q_{\theta r\theta}{}^p, zq_{\theta r\theta}{}^p \end{Bmatrix}\mathrm{d}z + \int_{\frac{h_e}{2}}^{\frac{h_e}{2}+h_p} \frac{\cos\left(\frac{\pi}{h_p}\rho\right)}{(R+z)}\begin{Bmatrix} e_{\theta r\theta}{}^p, \binom{R}{+z}e_{\theta r\theta}{}^p, ze_{\theta r\theta}{}^p, q_{\theta r\theta}{}^p, \\ (R+z)q_{\theta r\theta}{}^p, zq_{\theta r\theta}{}^p \end{Bmatrix}$$

$$\{A_{29}, A_{30}, A_{31}\} = \int_{-\frac{h_e}{2}-h_p}^{-\frac{h_e}{2}} \frac{[\cos\left(\frac{\pi}{h_p}\rho\right)]^2}{(R+z)}\{\epsilon_{\theta\theta}{}^p, m_{\theta\theta}{}^p, \mu_{\theta\theta}{}^p\}\mathrm{d}z + \int_{\frac{h_e}{2}}^{\frac{h_e}{2}+h_p} \frac{[\cos\left(\frac{\pi}{h_p}\rho\right)]^2}{(R+z)}\{\epsilon_{\theta\theta}{}^p, m_{\theta\theta}{}^p, \mu_{\theta\theta}{}^p\}\mathrm{d}z$$

$$\{A_{32}, A_{33}, A_{34}, A_{35}, A_{36}, A_{37}\} = \int_{-\frac{h_e}{2}}^{+\frac{h_e}{2}} \frac{E}{2(1+\upsilon)}l'^2\frac{1}{2(R+z)}\{1, \frac{1}{R+z}, \frac{z}{R+z}, \frac{1}{(R+z)^2}, \frac{z}{(R+z)^2}, \frac{z^2}{(R+z)^2}\}dz + \int_{-\frac{h_e}{2}-h_p}^{-\frac{h_e}{2}} \frac{E}{2(1+\upsilon)}l'^2\frac{1}{2(R+z)}\{1, \frac{1}{R+z}, \frac{z}{R+z}, \frac{1}{(R+z)^2}, \frac{z}{(R+z)^2}, \frac{z^2}{(R+z)^2}\}dz + \int_{\frac{h_e}{2}}^{\frac{h_e}{2}+h_p} \frac{E}{2(1+\upsilon)}l'^2\frac{1}{2(R+z)}\{1, \frac{1}{R+z}, \frac{z}{R+z}, \frac{1}{(R+z)^2}, \frac{z}{(R+z)^2}, \frac{z^2}{(R+z)^2}\}dz.$$